International Conference on Case Histories in Geotechnical Engineering

(1988) - Second International Conference on Case Histories in Geotechnical Engineering

03 Jun 1988, 10:00 am - 5:30 pm

Compaction-Induced Distress of a Long-Span Culvert Overpass Structure

Raymond B. Seed
Berkeley, California

Chang-Yu Ou
Berkeley, California

Recommended Citation

Compaction-Induced Distress of a Long-Span Culvert Overpass Structure

Raymond B. Seed
Berkeley, California

Chang-Yu Ou
Berkeley, California

SYNOPSIS: Compaction of backfill produces soil stresses and earth pressures which are not amenable to analysis by conventional methods. These compaction-induced earth pressures can produce stresses and deformations in flexible buried culvert structures which may significantly affect the stability and performance of these structures. This paper presents the results of a study in which deformations of a long-span flexible metal culvert were measured during carefully monitored backfill operations. These field measurements were then compared with the results of finite element analyses in order to investigate (a) the influence of compaction effects on culvert stresses and deformations, and (b) the ability of recently developed finite element analysis procedures to accurately model these compaction effects. The structure being monitored suffered excessive and unacceptable deformations which were shown to be primarily the result of compaction effects; these were well modelled by the analyses performed.

INTRODUCTION

This paper presents the results of a study in which deformations of a large-span flexible metal culvert structure were measured during backfill operations. Detailed records were maintained of backfill placement procedures and deflections were monitored at various stages of backfill placement. This case study was similar to an earlier study of a similar long-span culvert overpass structure (Seed & Ou, 1987) except that compaction procedures for the earlier study were carefully controlled in order to minimize the influence of compaction on structural deformations, whereas in this current study compaction procedures were not strictly controlled and poor backfill placement procedures led to large and unacceptable structural deformations.

Two types of finite element analyses were performed to model field conditions: (a) conventional analyses which are well able to model incremental placement of backfill in layers but which cannot model compaction-induced stresses and deformations, and (b) analyses incorporating recently developed models and analytical procedures which do permit modelling of compaction effects (Seed & Duncan, 1986). Comparison of the results of these two types of analyses with each other, as well as with the field measurements, provides a basis for assessing: (a) the potential importance of considering compaction effects in analyzing culvert stresses and deformations, and (b) the accuracy and usefulness of the new analytical methods for modelling compaction effects.

THE VISTA CULVERT STRUCTURE

The Vista culvert structure is located in Vista City, California, and is designed to perform as a two lane bridge over a small river. Figure 1(a)

shows a cross-section through the structure. The culvert is a low-profile arch with a span of 38 feet 5 inches, a rise of 15 feet 9 inches and a length of approximately 90 feet, founded on 3-foot high reinforced concrete stem walls with a reinforced concrete base slab. The culvert consists of 9 x 2-1/2-inch corrugated aluminum
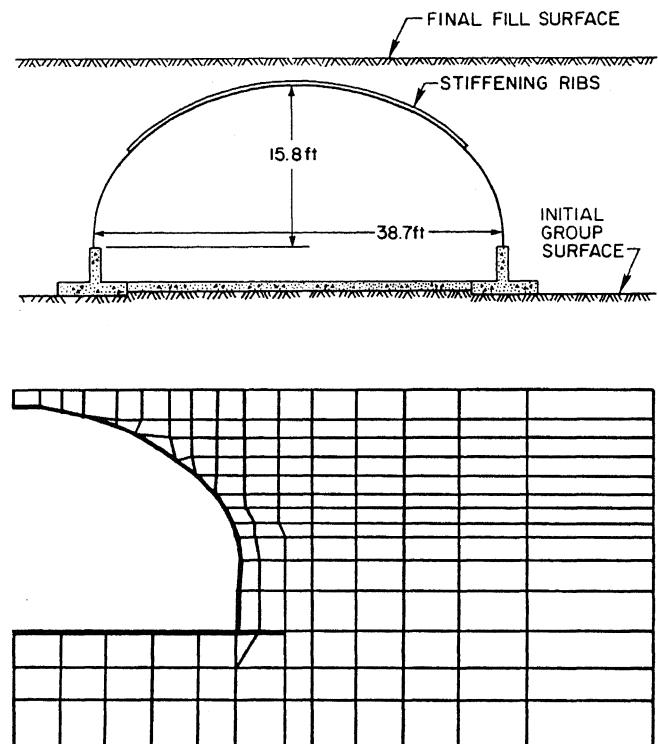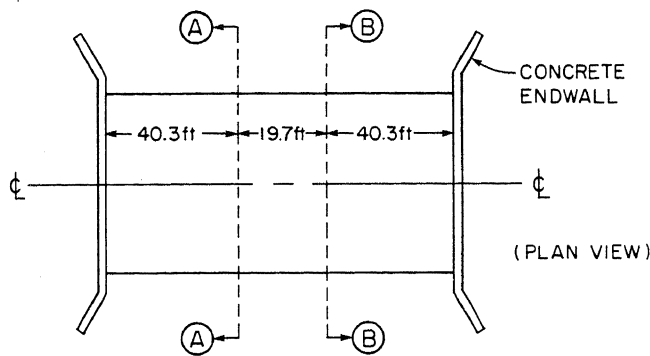

Fig. 1 The Vista Culvert Structure

Fig. 2 Measurement of Culvert Deformations

Culvert deformations were monitored at two cul-
vert sections during backfill placement and com-
paction. As shown in Figure 2(a), these sections
(A-A and B-B) were separated by approximately 20
feet and were both located approximately 40 feet
from the ends of the culvert to avoid any in-
fluence of restraint provided by the two rein-
forced concrete endwalls. At both cross sec-
tions, the displacements of 13 measurement
points were monitored relative to a pair of
reference points at the base of the culvert
haunches, as illustrated in Figure 2(b). The
change in span between the two reference points
was also measured, and all relative displace-
ments were corrected accordingly. Monitoring
the relative displacements of these fifteen
points permitted determination of the deformed
shape of each of the full cross sections at any
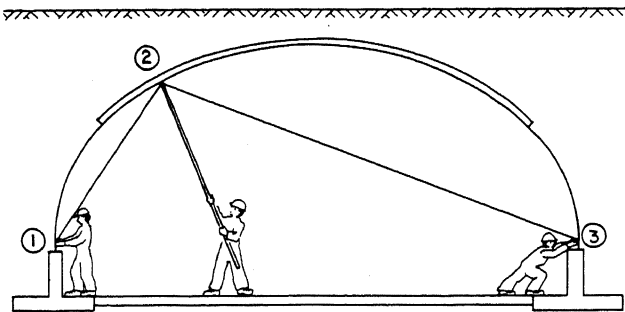given stage of backfill operations.

The distances between the measuring points and
each of the two reference points at each section
were measured using lightweight steel tapes.
The measuring points were permanently establish-
ed by means of marker bolts, and the ends of the
steel tapes were held to the ends of these bolts
by means of a fixture at the end of a pole which
was designed to mate consistently with the mea-
suring points. Tape tension was kept constant,
and no correction was made for thermal expansion
or contraction of the tape because the estima-
ted maximum correction was less than 1/16 inch
under the least favorable conditions encountered.
Numerous practice measurements were taken before
backfill operations began until it was demon-
strated that all measurements could be repeated
consistently within + 3/32-in. At the end of
each day of construction operations a number of
the most recent measurements were repeated at
random to verify that this level of measurement
accuracy was maintained.

No special steps were taken to control backfill
operations, but it was found that measured de-
formations of Sections A-A and B-B were very
similar at all backfill stages, as illustrated
by Figure 3 which shows the final deformed cul-
vert shapes at both measured sections upon com-
pletion of backfill placement and compaction.
Throughout the remainder of this paper, all "mea-
sured" deformations reported will represent aver-
aged deformations for the two measured sections.

structural plate 0.2 inches thick, and the crown
section is reinforced with Type IV aluminum bulb
angle stiffener ribs which occur at a spacing of
18 inches. The culvert haunches are grouted
into a slot at the top of the stem walls, pro-
viding a rigid connection for moment transfer at
this point.

The existing foundation soil at the site was a
non-plastic silty sand (SM). The existing silty
sand was used as backfill and was compacted to a
minimum of 95% of the maximum dry density deter-
mined by a Standard Proctor Compaction Test
(ASTM 698-D). Backfill placement and compaction
procedures will be discussed later in detail.
The final depth of soil cover over the crown of
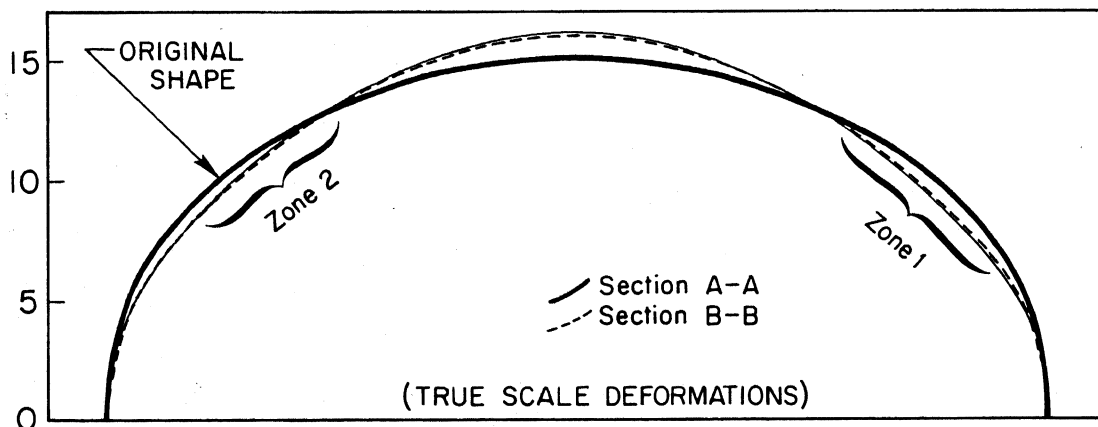the structure was approximately 2 feet.

Fig. 3 Final Deformations of the Vista Culvert at Measurement Sections A-A and B-B

The large inward radial deflections at the upper quarter point regions shown in Figure 3 were considered excessive and unacceptable, as they represented "flattening" and even minor reversal of curvature in these key regions. This, in turn, led to concerns regarding long-term stability. Accordingly, the last five feet of backfill were removed, allowing the culvert to "rebound". The upper backfill was the replaced and compacted using light compaction equipment in order to minimize deformations. This resulted in an acceptable final culvert configuration.

Figure 4 shows measured deformations at three backfill stages: (a) backfill midway up the haunches, (b) backfill approximately 1.5 feet below the crown, and (c) the final soil cover depth of 2.0 feet. In Figure 4, deformations are exaggerated by a factor of 5 for clarity. The general pattern of culvert deformations consisted of decreasing span and inward flexure of the quarter points at the juncture of the haunch and crown sections with increasing fill height, accompanied by an upward movement of the crown ("peaking"). The backfill elevation was carefully maintained at nearly the same level on both sides of the culvert at all fill stages, and placement and compaction operations were sufficiently similar on both sides of the culvert at any given fill stage that deformations
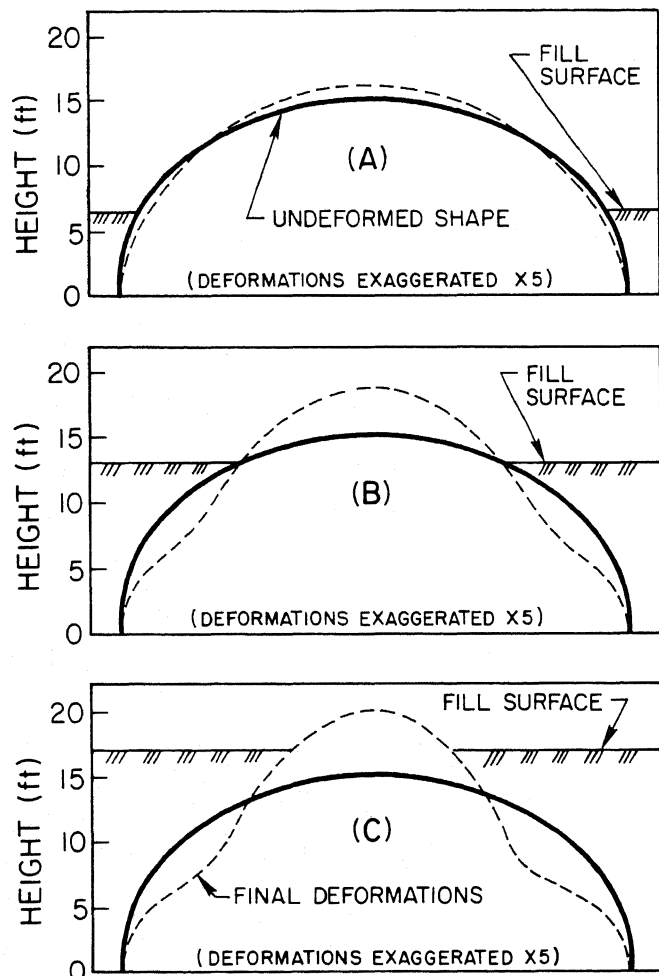

Fig. 4 Measured Deformation at Three Stages

of both sides of the culvert were largely symmetric as shown in Figure 4. Maximum peaking of the crowns of both measured culvert sections was approximately 12.5 inches, and the maximum inward radial deflection at the upper haunches was approximately 9 inches.

The measured culvert deformations can be well characterized by monitoring the vertical deflection of the crown point and the radial deformation of the quarter point, as shown in Figures 4 and 5. In Figure 5, which shows crown and quarter point deflections as a function of backfill level, it can be seen that as backfill was placed above the crown of the structure, peaking reversed and the crown began to descend slightly under the weight of the new crown cover fill.

OBSERVATIONS DURING BACKFILL PLACEMENT

The most important factors affecting the magnitude of compaction-induced earth pressures around the perimeter of the culvert are the contact pressure, footprint geometry and closest proximity to the point of interest achieved by any given compaction (or other construction) vehicle at any stage of backfill placement (Seed & Duncan, 1986). In order to properly model compaction-induced earth pressures acting against the culvert, it was thus necessary to continuously monitor the closest proximity to the culvert achieved by each construction vehicle at each stage of backfill placement and compaction, and field observers maintained a detailed and continuous record of this.

Six types of construction equipment were used during backfill operations: (a) a CAT D8H tracked dozer, (b) a CAT 824B rubber-tired dozer, (c) a CK780 backhoe/blade with four rubber wheels, (d) a 4,500-gallon water truck, (e) a two-drum vibratory hand roller, and (f) a single-drum vibratory roller pulled by a small Bobcat tractor. Fill was brought to the site in dump trucks, but these trucks never passed near to the structure.

Long-span "flexible" culverts are known to be susceptible to compaction induced deformations. Accordingly, it is common practice to require that only light hand compaction equipment operate in close proximity to the structure, while larger vehicles operate at some larger distance from the structure. Unfortunately, these requirements are sometimes poorly enforced and/or poorly understood by the contractor placing the fill. This was the case for this project.

Initially, as fill was placed at the lower haunches, only the small hand compactor operated within four feet of the structure, and the dump trucks and large water truck were kept at least 8 feet from the structure, even when operating as compactors. The zone 3 to 8 feet from the structure was compacted with the medium-sized rubber-tired vehicles.

At later backfill stages, however, as the fill reached the upper quarter point region, the contractor began to increasingly encroach on the structure with larger vehicles. This, in turn, led to a significant increase in compaction-induced earth pressures against the culvert and compaction-induced culvert deformations. At a fill stage of approximately 2 feet below the

crown, the large water truck passed to within very close proximity of the culvert (about 3-foot separation) along both sides of the structure. This produced readily noticeable plastic deformations which can be clearly seen in Figure 5. The contractor was promptly warned at this point, and no further instances of extremely large vehicle loads passing in close proximity to the structure occurred. Relatively large vehicles, including the CAT 824B and the CK780 did, however, continue to be used to compact inadviseably close to the structure (to within 2 to 3 feet of the structural plate) in this upper quarter-point fill region.

The degree of compaction achieved has only a minor effect on the magnitude of soil stresses induced by compaction but has a significant influence on the stiffness of the backfill. For this reason it was also necessary to closely monitor the degree of compaction achieved at all points in order to properly model backfill stress-deformation behavior in the finite element analyses performed. Based on constant observation of field operations, as well as 14 in-situ density tests, it was judged that the average density achieved was approximately 96% of the Standard Proctor maximum dry density at an average water content of approximately 7%. Density and water content variations were judged to be small.
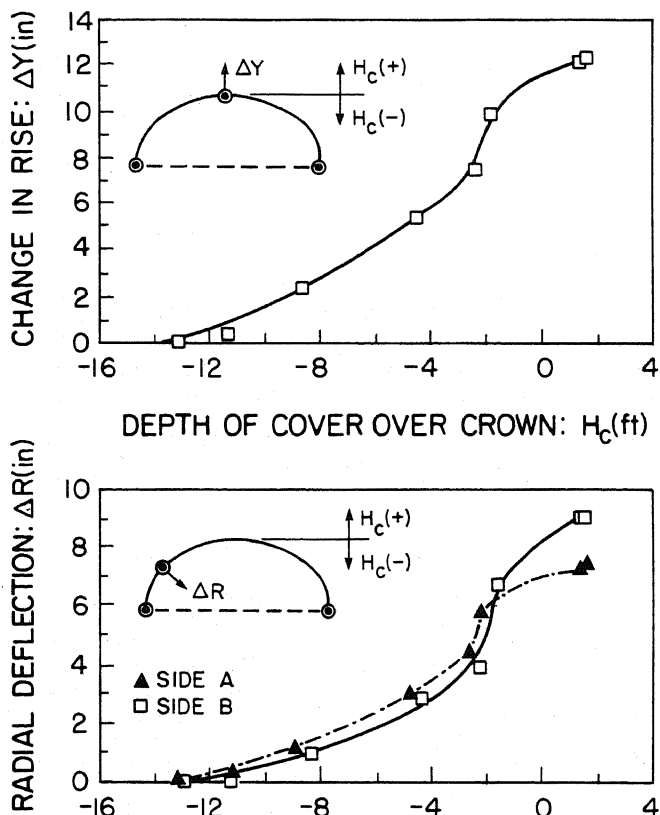

Fig. 5 Measured Deformations vs. Fill Height

FINITE ELEMENT ANALYSES PERFORMED WITHOUT MODELLING COMPACTION-INDUCED STRESSES

Two types of finite element analyses were performed in order to evaluate the significance of compaction effects on culvert deformations and stresses: (a) conventional analyses without any capacity for consideration of compaction-induced stresses, and (b) analyses incorporating recently developed finite element models and algorithms allowing consideration of compaction-induced soil stresses and associated deformations.

Both types of analysis used the hyperbolic formulation proposed by Duncan et al. (1980) as modified by Seed and Duncan (1983) to model non-linear stress-strain and volumetric strain behavior of the soils involved, varying the values of Young's modulus and bulk modulus in each soil element as a function on the stress state within that element at any given stage of the analysis.

The conventional analyses, without compaction effects, consisted of modelling placement of fill in successive layers or increments. A two-iteration solution process was used for each increment to establish appropriate soil moduli in each element in order to model nonlinear soil behavior. These analyses were performed using the computer program SSCOMP (Seed & Duncan, 1984), a two-dimensional plane strain finite element code.

Figure 1(b) shows the finite element mesh used for these analyses. Only one-half of the culvert and backfill was modelled because of the symmetric nature of both the backfill operations and the measured deformations. Soil elements were modelled with four-node isoparametric elements and the culvert structure and underlying concrete members were modelled with piecewise-linear beam elements. Nodal points at the right- and left-hand boundaries of the mesh were free to translate vertically, but were rigidly fixed against rotation or lateral translation, providing full moment transfer at the culvert crown and the centerline of the concrete base slab.

The program SSCOMP models all structural elements as deforming in linear elastic fashion, and this was appropraite as calculated structural stresses remained within the linear elastic range. Structural properties used to model the various components of the culvert structure were based on large-scale flexural test data, and are listed in Table 1.

TABLE 1. Structural Properties Modelled

Structural Component	E (kips/ft^2)	I (x10^4) (ft^4/ft)	Area (ft^2/ft)
Concrete Sections	464,000	0.75	352.0
Haunches (No Ribs)	1,468,000	0.0194	0.774
Crown (Rib)	1,468,000	0.0282	3.98

A series of isotropically consolidated, drained triaxial tests with volume change measurements were performed on samples of the backfill soil. Samples were compacted to approximately 95% of the Standard Proctor maximum dry density, taken

1186

as representative of field conditions, and were tested at effective confining stresses of between 7.6 and 21.8 psi. Figure 6 shows the results of these tests, as well as the modelled soil behavior based on the following hyperbolic soil model parameters: γ = 126 pcf, c = 0, ϕ = 38.6°, $\Delta\phi$ = 7.2°, K = 730, n = 0.3, R_f = 0.85, K_b = 200, m = -0.1, and K_{ur} = 1100. Modelled stress-strain behavior is in excellent agreement with the test results. Modelled volumetric strain behavior agrees well with the test data at low stress levels, but diverges at higher stress levels because the hyperbolic soil model used cannot model dilatency.

The open squares in Figure 7 illustrate the results of incrementally modelling fill placement without compaction-induced stresses using the program SSCOMP. As shown in this figure, calculated culvert displacements at the crown point are only approximately 40 percent of the measured values at all fill stages, and the maximum calculated radial deflection of the quarter point is less than one-fifth of that measured in the field. It is unlikely that this magnitude of discrepancy between deformations calculated without consideration of compaction effects and the actual field measurements is due to poor modelling of soil or structural stiffnesses, as these are all based on reliable test data, and it thus appears likely that compaction-induced earth pressures significantly influenced the measured field deformations.
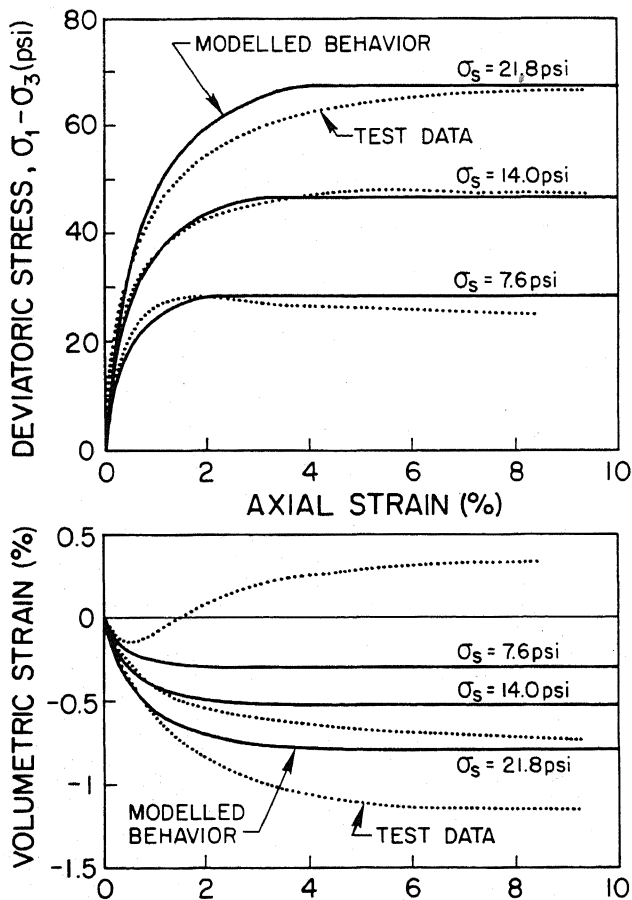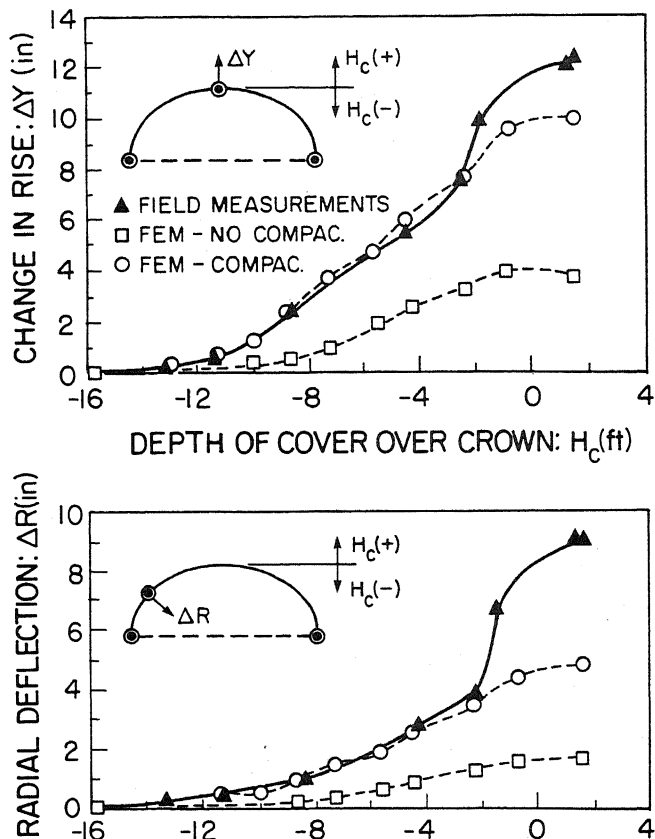

Fig. 7   Measured Culvert Deformations vs. Values Calculated With and Without Compaction

FINITE ELEMENT ANALYSES WITH MODELLING OF COMPACTION EFFECTS

A second set of finite element analyses were performed, this time using the program SSCOMPN (Ou, 1987), to model the effects of compaction-induced earth pressures. These analyses again incrementally modelled the placement of backfill in layers, but after each backfill placement increment an additional two-iteration solution increment was used to model the effects of compaction operations at the surface of the new backfill layer. The models and analytical procedures used to simulate compaction effects are described in detail by Seed and Duncan (1987), and a slightly modified hysteretic stress-path model developed by Ou (1987) was incorporated in these analyses. As these are unfortunately rather complex, only a brief general description follows.

Two soil behavior models are employed in these analyses. Nonlinear stress-strain and volumetric strain behavior is again modelled with the hyperbolic formulation used for the conventional analyses without compaction. The second soil behavior model is a model for stresses generated by hysteretic loading and unloading of soil. This hysteretic model performs two roles during analyses: (a) it provides a basis for the controlled introduction of compaction-induced soil stresses at the beginning of each compaction increment, and (b) it acts as a "filter," controlling and modifying the compaction-induced

Fig. 6   Modelled vs. Measured Soil Behavior

fraction of soil stresses during all stages of analysis.

Horizontal stresses within a given soil element are considered to consist of two types of fractions defined as: (a) geostatic lateral stresses ($\sigma_{x,o}$), which include all stresses arising due to increased overburden loads and deformations which results in lateral stress increases, and (b) compaction-induced lateral stresses ($\sigma_{x,c}$), which are the additional lateral stresses arising at the beginning of each compaction increment as a result of transient compaction loading. The overall lateral soil stress (σ_x) at any point is then the sum of the geostatic and compaction-induced stresses.

Compaction-induced lateral stresses are introduced into an analysis during "compaction" increments. Both the peak and residual compaction-induced lateral stresses at any point are modelled based on the peak, virgin compaction-induced horizontal stress increase ($\Delta\sigma_{x,vc,p}$) which is defined as the maximum (temporary) increase in horizontal stress which would occur at any given point as a result of the most critical positioning of any surficial compaction plant loading actually occurring if the soil mass was previously uncompacted (virgin soil). This use of $\Delta\sigma_{x,vc,p}$ allows consideration of compaction vehicle loading as a set of transient surficial loads of finite lateral extent which pass one or more times over specified portions of the fill surface, properly modelling the three-dimensional nature of this transient concentrated surface loading within the framework of the two-dimensional anlayses performed. The need to model the most critical positioning actually achieved by each compaction vehicle relative to each soil element at each backfill stage necessitated the constant monitoring of vehicle movements during backfill operations.

$\Delta\sigma_{x,vc,p}$, which is independent of previous hysteretic stress history effects, can be evaluated using 3-D linear elastic analyses, and is directly input for each soil element at the beginning of each compaction increment. The hysteretic soil behavior model then accounts for previous hysteretic loading/unloading cycles (e.g., previous compaction increments) and calculates both the actual peak and residual lateral stress increases on planes of all orientations within a soil element (residual vertical stress remains constant) based on $\Delta\sigma_{x,vc,p}$ and the previous hysteretic stress history of the soil element.

In addition to establishing the magnitudes of residual compaction-induced lateral stresses introduced at the beginning of each compaction increment (prior to nodal displacements and associated stress redistribution), the hysteretic soil behavior model also acts as a "filter," controlling and modifying the compaction-induced component of stress in soil elements at all stages of analysis. All calculated increases in σ_x at any stage during an analysis are considered to represent an increase in geostatic lateral stress and represent hysteretic "reloading" if a compaction-induced stress component is present. Subsequent to the solution of the global stiffness and displacement equations for any incre-

ment, therefore, the resulting calculated increases in σ_x are used as a basis for calculating an associated decrease in the compaction-induced fraction of lateral stress ($\sigma_{x,c}$). This progressive erasure or "overwriting" of compaction-induced lateral stresses by increased geostatic lateral stresses results in an overall increase of σ_x less than the calculated increase in $\sigma_{x,o}$ for soil with some previously "locked-in" compaction-induced lateral stress component, and corresponds to hysteretic "reloading." When solution of the global stiffness and displacement equations results in a calculated decrease in σ_x, it is assumed that this decrease is borne by both the geostatic and compaction-induced fractions of the pre-existing lateral stress in direct proportion to their contributions to the overall lateral effective stress.

Compaction-induced lateral stress increases in a soil mass can exert increased pressure against adjacent structures, resulting in structural deflections which may in turn partially alleviate the increased lateral stresses. Multiple passes of a surficial compaction plant, however, continually re-introduce the lateral stresses relaxed by deflections and result in progressvie rearrangement of soil particles at shallow depths. In order to approximate this process with a single solution increment, both compaction-induced lateral stresses and the corresponding nodal point forces for a given compaction increment are assumed to represent "following" loading from the current ground surface down to the depth at which $\sigma_{x,c}$ exceeds $\sigma_{x,o}$. All soil elements above this depth are assigned neglible moduli, resulting in calculations of displacements at all locations as a result of compaction-induced lateral forces, but (a) no changes in soil stresses result from displacements in soil elements above the specified depth of "following" compaction loading, and (b) compaction-induced nodal forces in this upper region are also undiminished by deflections.

Four additional soil parameters are needed for the hysteretic model controlling compaction-induced soil stresses, and these may be evaluated by correlation with the soil strength parameters c and ϕ (Seed & Duncan, 1986; Ou, 1987). The model parameters used for this analysis were: $K_O = 0.38$, $c_B = 0.0$, $K_{1,\phi,B} = 4.32$ and $\alpha = 0.57$.

Calculation of the peak, virgin compaction-induced lateral stress ($\Delta\sigma_{x,vc,p}$) to be input into each soil element at the beginning of each compaction increment is a time-consuming process. In the "free field" away from the culvert, three-dimensional linear elastic analyses were performed using Boussinesq closed-form solutions to calculate the peak lateral stresses induced at any given depth by each piece of construction equipment. These vlaues were then enveloped to produce a single profile of $\Delta\sigma_{x,vc,p}$ vs. depth which was used for all soil elements occurring at a distance of more than 6 or 7 feet from the culvert at all fill stages.

For soil elements near the culvert it was necessary to carefully review the recorded field observations in order to model peak stresses arising as a result of the most critical positioning

1188

(closest proximity) achieved by each piece of compaction equipment at each fill level. Initially, at fill levels up to the top of the haunches, the small hand compactor controlled peak compaction-induced stresses ($\Delta\sigma_{x,vc,p}$) adjacent to the culvert. At fill levels above the haunches, however, larger vehicles began to exert increasing influence on values of $\Delta\sigma_{x,vc,p}$ for soil elements in the region of the quarter point midway between the haunch and crown.

The analyses performed with SSCOMPN used a non-linear structural behavioral model which modelled the same behavior in the elastic range as was used for the previous analyses without compaction modelling, but which modelled nonlinear deformation behavior in the inelastic stress ranges. Parameters were again based on larg-scale flexural test data.

The open circles in Figure 7 show the results of incrementally modelling both backfill placement and compaction. Modelling of compaction effects has resulted in significantly improved agreement between calculated and measured culvert deflections at all backfill stages, as compared to the earlier analyses without compaction. The calculated maximum crown rise (peaking) of 10 inches represents an increase of 150% over the maximum peaking of 4 inches calculated by conventional analyses without consideration of compaction effects, and is only about 20% less than the value actually measured. Modelling compaction effects also more than doubled the maximum calculated radial displacement of the quarter point to more than 5 inches. This new value is still considerably less than the value actually measured, but this is due in large part to the large inelastic inward radial deflections caused by the close approach of the large water truck to the structure at a fill stage of approximately 2 feet below the crown, as discussed previously. Until this point, agreement between calculated and measured deflections was nearly perfect.

Figure 8 shows culvert bending moments and axial thrust around the culvert perimeter following completion of backfill operations as calculated in both sets of finite element analyses performed (with and without compaction). In Figure 8(a) it can be seen that modelling compaction effects resulted in increased bending moments in both the crown and haunch regions. The increased positive crown moment results in a factor of safety of only 1.45, which is less than that allowed for design. This is not of serious concern for design purposes, however, as it is still below the level required for the onset of plastic yield and represents an increase in the ability of the crown section to withstand subsequent negative moments which will arise due to live traffic loads.

The increased bending moments at the top and base of the unreinforced haunch region are considerably more serious. Without compaction effects the calculated minimum factor of safety with regard to exceeding the plastic moment capacity in the haunch region was more than 2.5, apparently representing conservative design. Modelling compaction effects reduced this factor of safety to slightly less than 1.0 (FS = 0.93) at the top of the haunch region and FS = 1.8 at
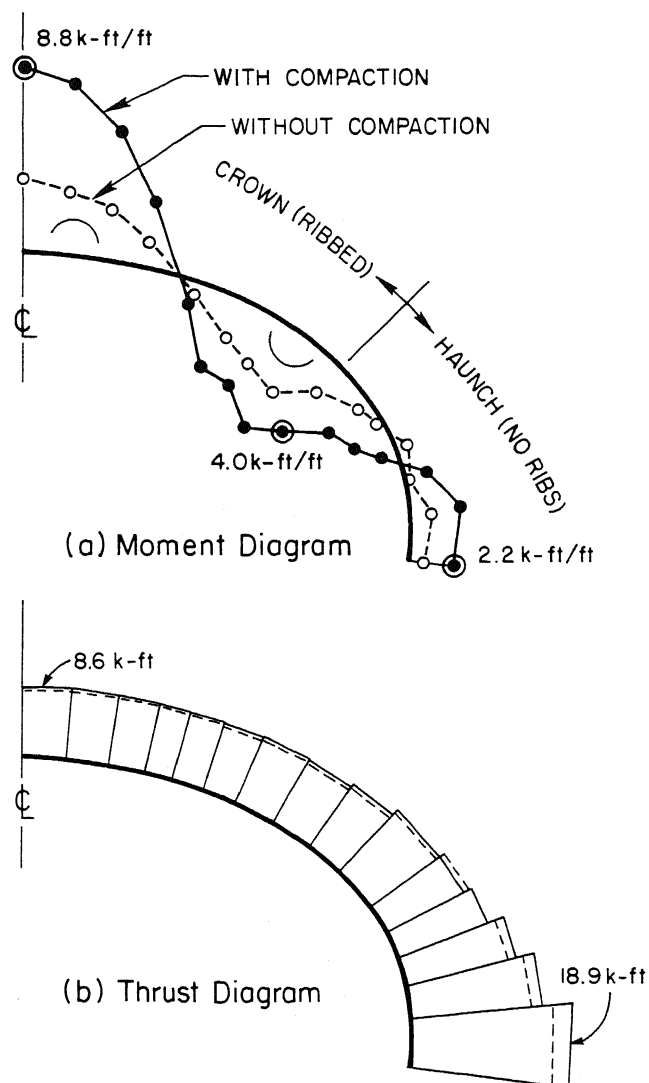

(a) Moment Diagram

(b) Thrust Diagram

Fig. 8 Calculated Culvert Bending Moments and Thrusts With and Without Compaction

the base, and both of these moments correspond to flexure in directions representing potential failure modes. These moments, together with the resulting unacceptable deformed shapes of the upper haunch and quarter point regions, led to the decision to excavate the last five feet of fill. This permitted the structure to rebound, and the backfill was then replaced using only light hand compaction equipment to minimize compaction-induced stresses and deformations. This resulted in an acceptable final structural configuration.

In Figure 8(b) it can be seen that modelling compaction-induced earth pressures resulted in calculation of only minor increases in thrust around the perimeter of the culvert. These increases, which were between zero and 15% around the culvert perimeter, were much less pronounced than was the effect of modelling compaction on calculated culvert bending moments.

1189

SUMMARY AND CONCLUSIONS

Two types of finite element analyses were performed as part of these studies: (a) conventional analyses which were well able to model incremental placement of backfill in layers, but which cannot model compaction-induced stresses and deformations, and (b) analyses incorporating recently developed behavioral models and analytical procedures which do permit modelling of compaction effects. The results of these analyses were compared with the field measurements of culvert behavior, and these comparisons showed that compaction-induced earth pressures resulting from poor backfill compaction procedures were the principal cuase of the unsatisfactory structural behavior observed. This conclusion was well-supported by the satisfactory culvert performance following excavation (and rebound) and careful recompaction of the upper backfill zone. In addition, these studies provided good support for the accuracy and effectiveness of the new behavioral models and finite element analysis procedures used to model the effects of soil compaction.

REFERENCES

Duncan, J.M., Byrne, P., Wong, K.S. and Mabry, P. (1980). "Strength, Stress, Strain and Bulk Modulus Parameters for Finite Element Analyses of Stresses and Movements in Soil Masses, Geotechnical Engineering Research Report No. UCB/GT/80-01, University of California, Berkeley.

Seed, R.B. and Duncan, J.M. (1983). "Soil-Structure Interaction Effects of Compaction-Induced Stresses and Deflections," Geotechnical Engineering Research Report No. UCB/GT/83-06, University of California, Berkeley.

Seed, R.B. and Duncan, J.M. (1984). "SSCOMP: A Finite Element Program for Evaluation of Soil-Structure Interaction and Compaction Effects," Geotechnical Engineering Research Report No. UCB/GT/84-02, University of California, Berkeley.

Seed, R.B. and Duncan, J.M. (1986). "Compaction-Induced Stresses and Deformations for Yielding Structures," Journal of the Geotechnical Engineering Division, ASCE, Vol. 112, No. 1, January.

Seed, R.B. and Ou, C.Y. (1987). "Measurement and Analysis of Compaction Effects on a Long-Span Culvert," Transportation Research Record, No. 1087, pp. 37-45, January.

Ou, C.Y. (1987). "Finite Element Analysis of Compaction-Induced Stresses and Deformations," Ph.D. Thesis, Stanford University, November.

1190